





Interface structure and mobility in martensitic shape memory alloys

W. Cai*, X.L. Meng, Y.F. Zheng, J.X. Zhang, L.C. Zhao

School of Materials Science and Engineering, Harbin Institute of Technology, Harbin 150001, China Received 22 April 2005; received in revised form 7 February 2006; accepted 9 February 2006

Abstract

The interface structure and its mobility in the martensites of shape memory alloys (SMAs) are reviewed. The emphasis is placed on the evolution of interface structure during deformation and the relations of interface characteristics to the mobility in cold-deformed TiNi-based alloys and the types, structure and mobility of interfaces in Cu-based SMAs. With the increase of deformation strain in the cold-deformed TiNi alloys, the interface type of martensite variants changes and their mobility becomes bad gradually. For the Cu-based SMAs, the A/C and A/B interfaces have effective mobility and may move smoothly and become straight during motion. On the contrary, the mobility is not effective for the A/D interface. © 2006 Elsevier B.V. All rights reserved.

Keywords: Shape memory alloy; Martensite; Interface structure; Mobility

1. Introduction

It is well known that the interface structures of martensite variants and their mobility play an important role in regard to the particular properties of shape memory alloys (SMAs) [1–3]. The characteristics and the mobility of various interfaces determine the recovery of the pre-deformation microstructure and the macroscopic shape upon heating and/or unloading, which correspond to the shape memory effect (SME) and pseudoelasticity. Thus, an understanding of the structure of the interfaces and their mobility are essential to a further understanding of shape memory behavior.

2. Interfaces and their mobility in martensite of TiNi-based SMAs

2.1. TiNi SMAs

The substructure of the TiNi intermetallic compound without deformation is predominantly $\langle 0\,1\,1\rangle_M$ type II twins and the intervariant interfaces are mainly $\{1\,1\,\bar{1}\}_M$ type I and $(1\,0\,0)_M$ compound twin related [4–6]. For the Ti–49.8 at.% Ni alloy, after slight cold deformation, the $(1\,0\,0)_M$ compound twinning intervariant boundaries become curved and irregular. Meanwhile the width of the internal $\langle 0\,1\,1\rangle_M$ type II twinning substruc-

tural bands inside each martensite variant shows no obvious change. Further increasing of the deformation strain (<16%), the substructural bands are found to adjust partially their orientation by the rearrangement of the internal twinning structure, and both the intervariant boundary and the substructural boundary of the martensite variants become confused and blurred. Simultaneously, some needle-like plates, as the subunit smaller than the $(0.11)_{M}$ type II twin related unit, appear obviously inside some substructural bands of martensite variants. It is also found that amount of $(1 \ 1 \ 1)_M$ type I twinning mode increases and some (011)_M type I twins form inside the coalesced substructural bands. The $(1 \ 1 \ 1)_{M}$ type I twinning interface is relatively straight, with locally one-atomic-height step existing at the boundary, whereas the $\langle 0 \ 1 \ 1 \rangle$ type II twinning interface is clearly distorted and partly loses its coherency. The (0 0 1)_M compound subtwinning interface is relatively straight with one-atomiclayer height step existing at the boundary, whereas the newly formed (011)_M type I subtwinning interface is also relatively straight, despite being stepped at local positions. Fig. 1 shows a high-resolution transmission electron microscopy (HREM) image of the residual intervariant (100)_M compound twinning boundary in the 16% deformed alloy, from which it can be seen that the $(001)_{M}$ compound twin related substructure develops inside each martensite variant. It causes the atomic combination at the intervariant interface complex and leads to a wavy interface structure, indicating that its mobility deteriorates.

When the alloy is deformed to 22%, $(001)_M$ compound, $(011)_M$ type I and $(111)_M$ type I twinning modes are found to form inside the substructural bands, and the $(111)_M$ type I

^{*} Corresponding author. Tel.: +86 451 86418649; fax: +86 451 86415083. *E-mail address:* weicai@hit.edu.cn (W. Cai).

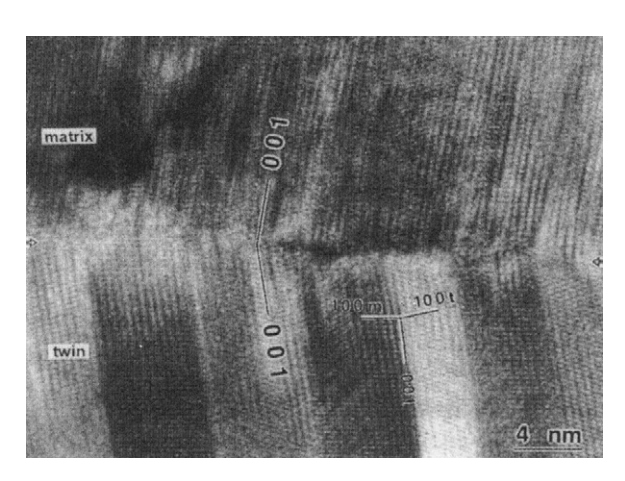


Fig. 1. HREM image of deformed martensite in the specimen deformed to 16% showing the $(1\,0\,0)_M$ compound twinning interface, electron beam// $[0\,1\,0]_{M,T}$.

twinning interface exhibits a wavy feature. Further increasing the deformation strain (over 30%), it is difficult to find out the original intervariant boundaries, which suggests that the substructural bands completely merge into each other. Lattice distortion is extreme in some areas and at local regions amorphous bands emerge in the specimen.

As mentioned above, during deformation, the quantities of the $(1\,0\,0)_M$ compound and $(0\,1\,1)_M$ type II twinning plates are reduced, with the increase of $(1\,1\,\bar{1})_M$ type I, $(0\,0\,1)_M$ compound and $(0\,1\,1)_M$ type I twinning bands and the introduction of $(1\,1\,1)_M$ type twinning plates. The $(1\,0\,0)_M$ intervariant bound-

ary becomes wavy and gradually loses its mobility with increasing the deformation strain. At the same time, the $\langle 0\,1\,1\rangle_M$ type II twinning boundary changes from the gradually and randomly curved one to the distorted one, the $(1\,1\,\bar{1})_M$ type I, $(0\,0\,1)_M$ compound and $(0\,1\,1)_M$ type I twinning boundaries becomes stepped, and the $(1\,1\,1)_M$ type I twinning boundary exhibits wavy feature, indicating that their mobility deteriorate during deformation.

2.2. Ti-Ni-Nb: wide-hysteresis SMAs

It has been shown [6–9] that the stress induced martensitic transformation is basically completed when the Ti_{46.3}Ni_{44.7}Nb₉ (numbers indicate at.%) alloy is deformed to 8% at 293 K. Fig. 2(a) shows a typical morphology of stress induced martensite (SIM) in 8% deformed specimen, with the corresponding electron diffraction patterns (EDPs) shown in Fig. 2(b). It is found that the SIM variants M_1 and M_2 are $(100)_M$ compound twin related. Fig. 2(c) is the HREM image of (100)_M compound twinning interface between M₁ and M₂. Obviously, the interface of the (100)_M compound twin is straight, well-defined and perfectly coherent. With increasing deformation strain, the ledges and distorted layers are observed in the (100)_M intervariant interface and interfacial coherence is damaged to some extent in the deformed SIMs. Fig. 2(d) shows a HREM image of (100)_M compound twinning interface between deformed SIM variants in the 16% deformed specimen. It is seen that there exists a distorted layer with about 3 nm width in the martensite variant interface and the interfacial coherence is

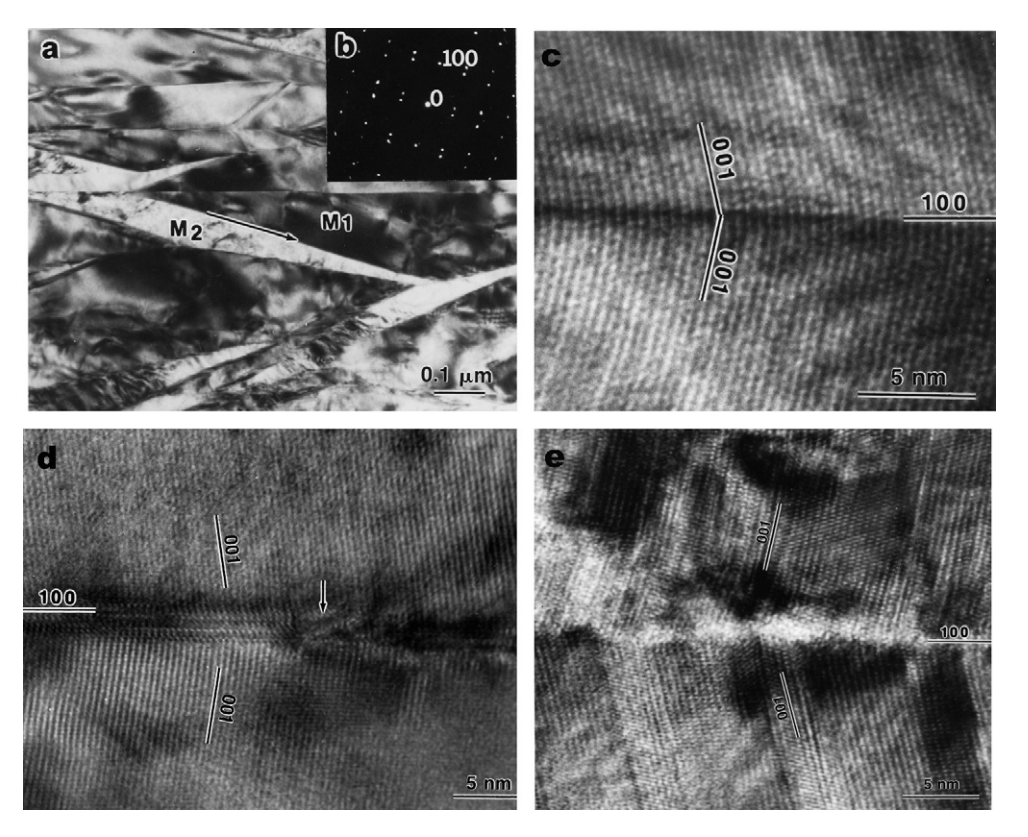


Fig. 2. (a) Bright-field image, (b) corresponding EDPs of two variants of two variants noted with arrow in (a), (c) HREM image of the $(1\,0\,0)$ twinning interface in the 8% deformed specimen, (d) HREM of $(1\,0\,0)_M$ twinning interface in the 16% deformed specimen, and (e) HREM image of $(1\,0\,0)$ twinning interface in the 24% deformed specimen in $Ti_{46.3}Ni_{44.7}Nb_9$ alloy.

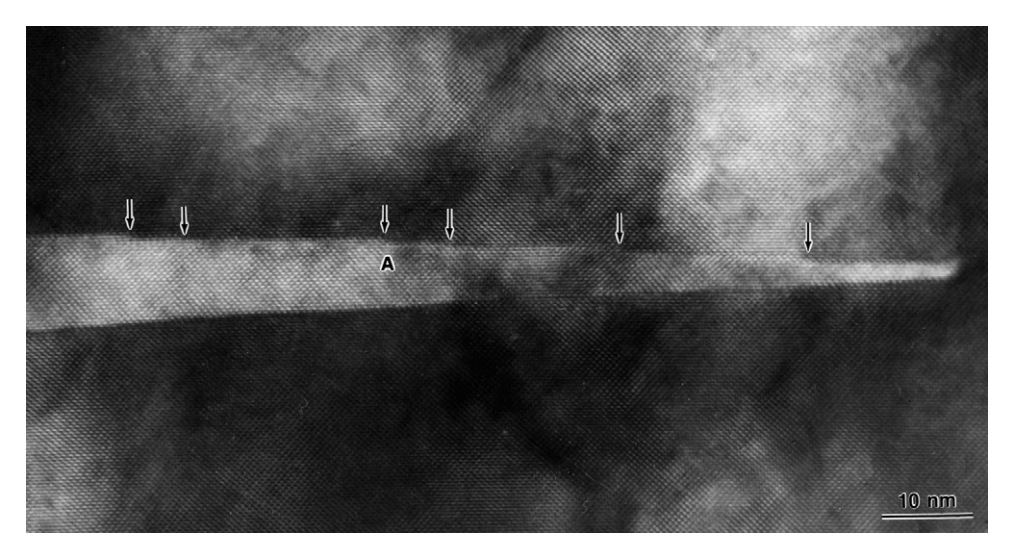


Fig. 3. HREM image of (011) type I twinning interface inside the deformed stress induced martensite in the Ti_{46.3}Ni_{44.7}Nb₉ alloy deformed to 16% at 293 K.

damaged. With further increasing the deformation strain, the ledges and distorted layer gradually develop into confused layers and the interfacial coherence is lost. Fig. 2(e) shows a HREM image of (100) compound twinning martensite variants interface in the $\rm Ti_{46.3}Ni_{44.7}Nb_9$ alloy deformed to 24% at 293 K. It is obvious that the interface is confused and exhibits an irregularly undulating configuration. There is no doubt that the mobility of the intervariant interface gradually declines during deformation.

In the $Ti_{46.3}Ni_{44.7}Nb_9$ alloy deformed to 8% at 293 K, the substructure of SIM variants is mainly $(1\ 1\ \bar{1})_M$ type I twins. The interface is straight and well-defined as well as perfectly coherent. Increasing the deformation strain to 16%, internal $(0\ 0\ 1)_M$ compound, $(0\ 1\ 1)_M$ type II and $(0\ 1\ 1)_M$ type I twins are also found within the substructure of the martensite. The ledges and distorted layers are observed in the $(0\ 1\ 1)_M$ type I twin interface and the interfacial coherence is damaged to some extent, as shown in Fig. 3. Clearly, some irregular ledges exist in the

 $(0\,1\,1)_M$ twinning interface as denoted by arrows. The distance of two adjacent ledges varies from 6 to 20 nm and the height is about 2–4 $(0\,1\,1)$ spacing. It was observed that the $(0\,1\,1)_M$ twinning boundary becomes stepped and partly loses its coherence.

2.3. Ti-Ni-Hf: high-temperature SMAs

The main substructures in a $Ti_{36}Ni_{49}Hf_{15}$ alloy are $(0\,0\,1)_M$ compound twins and $(0\,0\,1)_M$ stacking faults [10]. The intervariant interfaces are $(0\,0\,1)_M$ type I and $(0\,1\,1)_M$ type II twin related. Fig. 4 shows the HREM image of two neighboring martensite variants in the $Ti_{36}Ni_{49}Hf_{15}$ alloy. In the TiNiHf alloy the $(0\,0\,1)_M$ type I twinning interface is straight and well-defined, while the $(0\,1\,1)_M$ type II twinning interface is gradually and randomly curved. It has been reported that [11,12] that the mobility of intervariant interfaces in Ti–Ni–Hf alloy is very poor. During tensile deformation, the intervariant interface movement is difficult.

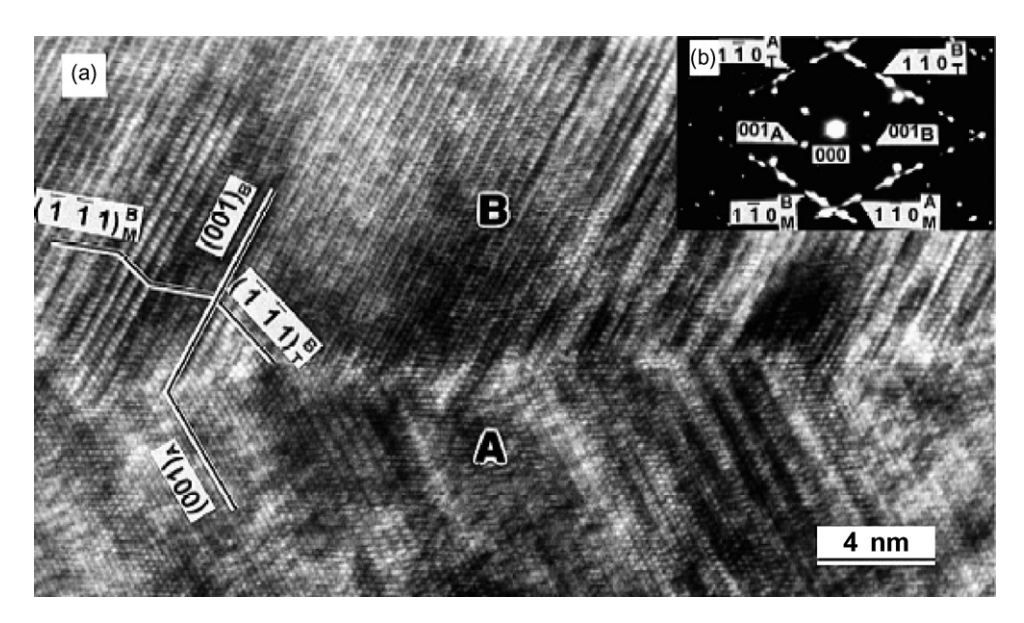


Fig. 4. (a) HREM image of the junction plane between two neighboring martensite variants and (b) its corresponding EDPs for Ti₃₆Ni₄₉Hf₁₅ alloy.

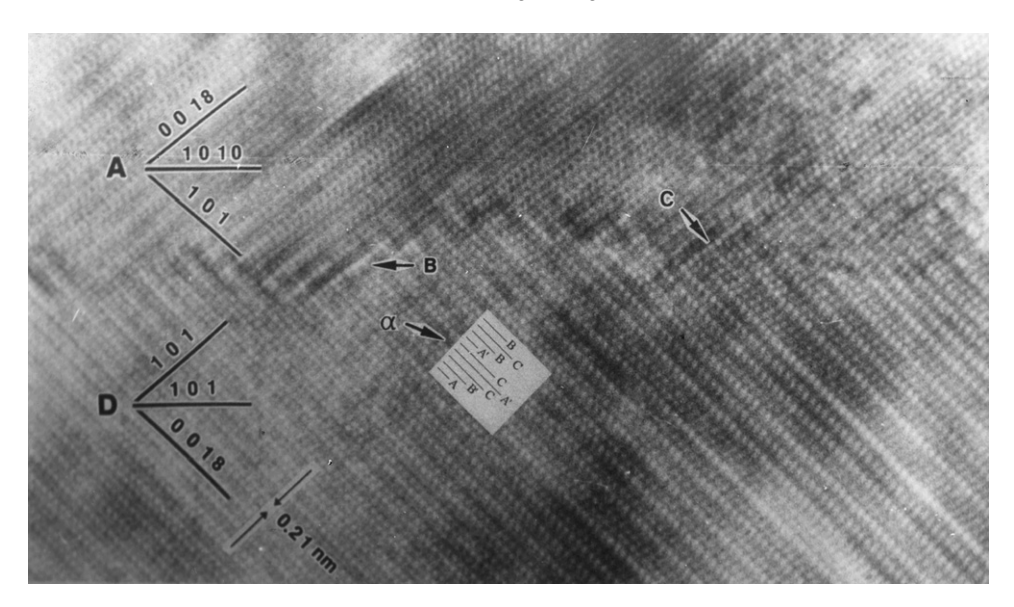


Fig. 5. Lattice image of A/D type interface in Cu-Zn-Al alloy.

3. Interfaces and their mobility in martensite of Cu-based SMAs

In Cu–Zn–Al alloys [2,13–15], there are three types of intervariant boundaries: A/B, A/C and A/D. HREM observations show that the A/C interface is quite straight, well-defined and perfectly coherent and the A/B interface is irrational, coherent and gradually curved. Fig. 5 is HREM image showing the $(1010)_{18R}$ A/D type twin boundary taken along the $[010]_{18R}$ zone axis. The upper variant appears misoriented, which may be due to the fact that the [0 1 0]_{18R} direction of the two variants are not exactly parallel. On an atomic scale, the A/D type boundary consists of irregularly serrated steps, with the facet parallel to the basal plane of one or the other variant. Along the facet there is a distorted area where the facet deviates from its corresponding basal plane (shown by arrows B, C), i.e. A basal plane stacking fault can be identified in martensitic variant D. Unfortunately, the other stacking faults cannot be distinguished from the stacking fault sequence due to the misorientation. There is no significant difference in the boundary orientation, no matter whether the stacking sequence in the martensite variant is perfect or a single fault is present. Therefore, the A/D interface is stepped, and the boundary steps are composed of the basal planes of the two variants.

In situ transmission electron microscopy (TEM) shows that A/B and A/C interfaces are mobile. Fig. 6(a)–(c) shows an example of motion of the A/B interface under tensile stress. During the initial stage, the boundary is not strongly activated by the external tensile stress; the observed phenomenon is only the adjustment of stacking fault contrasts. When the strain is about 1.5%, the boundary starts moving, while for a strain of about 3%, the width of variant A between two arrows decreases by 0.1 µm, as illustrated by the sequence of photographs in Fig. 6. At a low stress level, the movement is very smooth, but when the stress rises, the reaction of the boundary is different from segment to segment. That is, certain segments of the boundary move more easily than others, resulting in a wandering boundary. The movement of an A/C interface is similar to that of the A/B interface. During movement, the interface keeps straight and smooth. The stacking faults have no substantial influence on the movement of

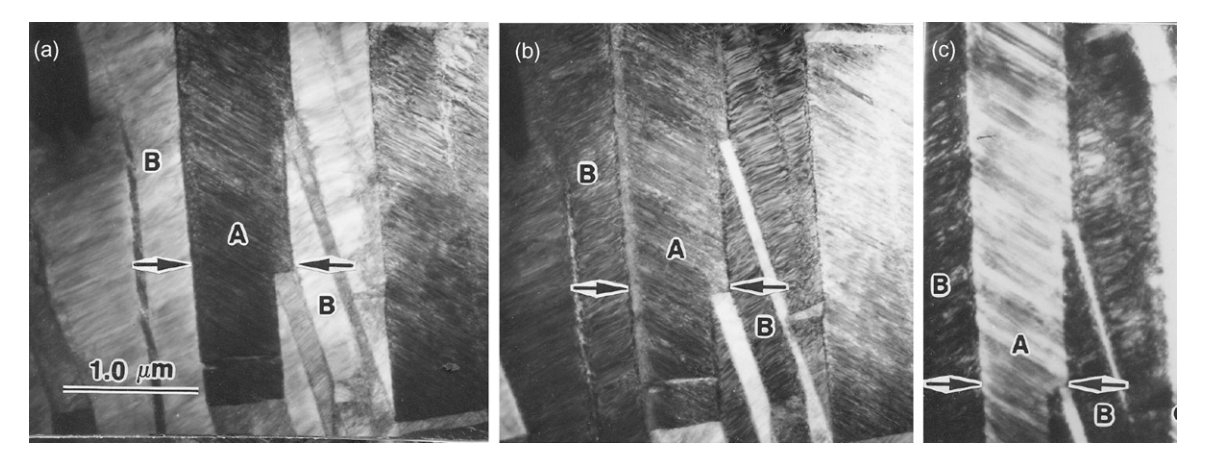


Fig. 6. TEM in situ observation of the movement of A/B interface due to tensile strain: (a) 0%, (b) \sim 1.5% and (c) \sim 3%.

the interfaces. No obvious movement of A/D interfaces is found during tensile by in situ TEM observation, showing that the A/D interface is immobile.

It is reasonable to conclude that the mobility is controlled by two factors: one is the degree of self-accommodation, and the other is the misorientation of the twin plane or matching plane. Nearly perfect self-accommodation and small misorientation results in the A/B and A/C interfaces having good mobility. The large misorientation of the matching planes in the A/D interface offers resistance to movement of the boundary though A/D pairs also show good self-accommodation.

4. Summary

- (i) With an increase of deformation strain in cold deformed TiNi alloys, the incidence of the $(1\,0\,0)_M$ compound and $(0\,1\,1)_M$ Type II twinned plates is reduced, with an increase of $(1\,1\,\bar{1})_M$ type I, $(0\,0\,1)_M$ compound and $(0\,1\,1)_M$ type I twinning bands and the introduction of $(1\,1\,1)_M$ type I twinned plates. The $(1\,0\,0)_M$ intervariant interface gradually loses its mobility and becomes wavy, the $(0\,1\,1)_M$ type II twinning boundary changes from a gradually and randomly curved one to a distorted one. The $(1\,1\,\bar{1})_M$ type I, $(0\,0\,1)_M$ compound and $(0\,1\,1)_M$ type I twinning boundaries become stepped, and the $(1\,1\,1)_M$ type I twinning boundary exhibits wavy features, indicating that their mobility is reduced with increasing deformation strain.
- (ii) The interface of SIM variants in Ti–Ni–Nb alloy is straight and well-defined as well as coherent. However, ledges and distorted layers are formed in the interface of stress induced martensites subjected to low deformation strain and the interfacial coherence is damaged. With an increase of deformation strain, the ledges and distorted layers gradually turn into confused layers and the interfaces of martensite variants completely lose coherence. The deformation gives rise to lattice distortion and damages interfacial coherence in deformation-induced martensites, resulting

- in the deterioration of interfacial mobility. The intervariant interface in TiNiHf alloy exhibits poor mobility.
- (iii) In CuZnAl alloy, the A/C interface is straight, well-defined and perfectly coherent. The A/B interface is irrational, coherent and gradually curved. The A/D interface is stepped, and the boundary steps are composed of the basal planes of the two variants. The A/C and A/B interfaces have effective mobility and may move smoothly and remain straight during movement. On the contrary, the mobility is restricted for the A/D interface.

Acknowledgement

The present work was supported by National Nature Science Foundation of China (nos. 50471018 and 50531020).

References

- [1] K. Otsuka, Jpn. J. Appl. Phys. 10 (1971) 571.
- [2] J.X. Zhang, Y.F. Zheng, Y.C. Luo, L.C. Zhao, Acta Mater. 47 (1999) 3497.
- [3] M. Nishida, C.M. Wayman, A. Chiba, Metallography 21 (1988) 275.
- [4] Y.F. Zheng, B.M. Huang, J.X. Zhang, L.C. Zhao, Mater. Sci. Eng. A 279 (2000) 25.
- [5] Y.F. Zheng, L.C. Zhao, H.Q. Ye, Mater. Sci. Eng. A 297 (2001) 185.
- [6] L.C. Zhao, W. Cai, Y.F. Zheng, Mater. Sci. Forum 394/395 (2002) 185.
- [7] L.C. Zhao, Mater. Sci. Forum 327/328 (2000) 23.
- [8] Y.F. Zheng, W. Cai, J.X. Zhang, L.C. Zhao, H.Q. Ye, Acta Mater. 48 (2000) 1409
- [9] L.C. Zhao, Y.F. Zheng, W. Cai, Intermetallics 13 (2005) 281.
- [10] Y.F. Zheng, W. Cai, J.X. Zhang, Y.Q. Wang, L.C. Zhao, H.Q. Ye, Mater. Lett. 36 (1998) 142.
- [11] F. Dalle, E. Perrin, P. Vermaut, M. Masse, R. Portier, Acta Mater. 50 (2002) 3557
- [12] X.L. Meng, W. Cai, L.M. Wang, Y.F. Zheng, L.C. Zhao, L.M. Zhou, Sci. Mater. 45 (2001) 1177.
- [13] J.X. Zhang, Y.F. Zheng, L.C. Zhao, Acta Mater. 47 (1999) 2125.
- [14] W. Cai, J.X. Zhang, Y.F. Zheng, L.C. Zhao, J. Phys. IV 112 (2003) 519
- [15] J.X. Zhang, Y.F. Zheng, W. Cai, L.C. Zhao, Acta Metall. Sin. 10 (1997) 425.